A Computational Study on the Stability of Dapdiamide D Conformers

R. Majdan-Cegincara[a,*], R. Ghadari[b] and R. Hosseinzadeh-Khanmiri[a]

aDepartment of Chemistry, Tabriz Branch, Islamic Azad University, Tabriz, Iran

bComputational Chemistry Laboratory, Department of Organic and Biochemistry, Faculty of Chemistry, University of Tabriz,

5166616471 Tabriz, Iran

The conformational analysis of the organic compounds specially the biologically active natural products has attracted the consideration of different research groups. Therefore, in the present study the MP2/6-311+g(d,p)//B3LYP/6-311+g(d,p) level of theory was used to study the conformations of dapdiamide D. The identity of interactions in selected conformers was studied using atom in molecule approach. The energies of hydrogen bonding and Van der Waals interactions were calculated using the potential energy density $V(r)$ at the bond critical point. An interaction between carbonyl and nitrogen of the amide functional group is evident, in most of the cases. This interaction creates a boat-like seven member-ring. The interaction between amine and hydrogen of the amide functional groups is important as well. This interaction forms a five-member ring. The results showed that the potential energy density $V(r)$ and electron density at the bond critical points can be used as a criteria to determine the strength of the interactions.

Keywords: Conformations analysis, Dapdiamide

INTRODUCTION

The dapdiamide A-E were used as antibiotic. These compounds were extracted from *Pantoea agglomerans* by Dawlaty and co-workers [1] (Fig. 1). This strain produces different types of the antibiotics [2-5]. The dapdiamides (DAP) are active against *Erwinia amylovora*, as well. This bacterium is the reason for the plant disease "fire blight".6,7 The dapdiamides are structurally similar to the methoxyfumaroyl-DAP dipeptides and they show a broad spectra of antibacterial activity *via* the targeting of glucosamine-6-phosphate (GlcN-6-P) synthase [8,9].

Using the computational approach is an ongoing way to study organic compounds [10-13]. Especially, finding the low-energy conformations of the organic compounds is very important and different studies have been carried out in this respect [14-17]. As an example, Arabieh and co-workers studied the low-energy conformers of the pamidronate. The

mentioned compound is a well-known pharmaceutical to treat bone diseases [18]. Conformational study of the methyl cyanoacetate and cyanoacetic acid were carried out by Reva *et al*. Their results showed that these two systems have nearly isoenergetic conformers [19]. Dowd and co-workers aimed the study of the carbohydrate compounds. They developed a Monte Carlo-based procedure to examine the conformations of the carbohydrates *via* a torsion angle-based search [20]. An optimization method to calculate the energy of polypeptides was reported by Lee and co-workers. This method was used successfully to find the global minima [21]. Structural analysis of the α/β peptides including *cis-β*-aminocyclopropane carboxylic acids was reported by De Pol and *et al*. [22]. Introducing new and stable foldamers and oligopeptides in solution [23-25], is the key to introduce structurally well-defined peptide units. Conformational analysis of the neutral, protonated, and deprotonated glutamine in gas phase was reported, as well. In this study different properties, including hydrogen bonding, relative electronic energies, zero point vibrational

---

*Corresponding author. E-mail: majdan@iaut.ac.ir
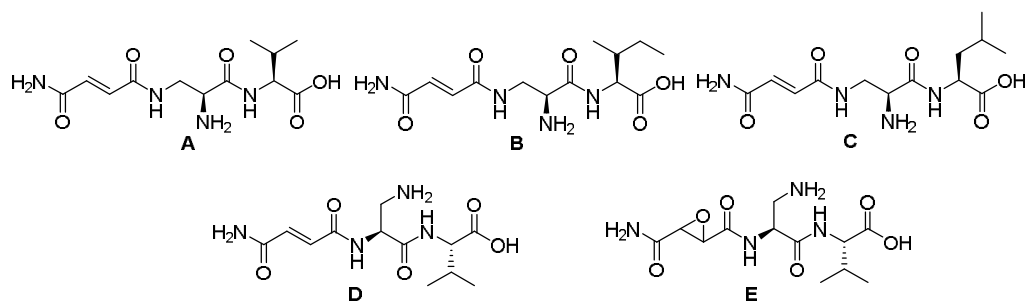
Fig. 1. An antibiotic family dapdiamide (A-E).

energies, and other properties were investigated [26]. Hydrogen bonding in the amino acids have attracted the consideration of the Ramaniah and co-workers, too [27]. In drug like molecules, the inter- or intra-molecular hydrogen bonding is very important. The intra-molecular interactions will affect the functional groups which could contact with the solvent or biomolecular targets [28]. Because of the above-mentioned importance of the dpadiamid family and intramolecular interactions, we have studied the relationship between energy of the conformers and intramolecular interactions. All calculations have been carried out in the gas phase, making us sure from the absolute effect of the intramolecular interactions without the effect of media such as solvent.

COMPUTATIONAL METHOD

The Avogadro (1.1.0) program was used to draw the structure of the investigated molecule. Conformational search was done using the same program. Molecular mechanics with Open Babel's force fields (OBForceFieldMMFF94) was used to do the conformational search. Random rotor search algorithm employed in the Avogadro program was used. All of the single bonds including amide bonds were considered free to rotate. Finally 83,365 conformations were obtained [29]. To optimized the structures Gaussian 09, revision A. 01 package was used [30]. The B3LYP/6-31G(d,p) level of theory is an acceptable choice to compute the accurate thermodynamic parameters for intramolecular interactions.[31] Therefore, in this study the mentioned level of theory was used for optimizing the structures and frequency calculations. The absence of imaginary frequencies was used to confirm the minimum nature of stationary points. The MP2/6-311+g(d,p) level of theory was used to do single point calculation as well as NBO analysis. CYLview program was used as the graphical interface to create the three dimensional images of the optimized structures [32]. The Multiwfn (ver. 3.3.5) [33,34] was used for AIM [35,36] studies. The hydrogen bond energy was calculated by approach suggested by Espinosa and co-workers. They used the potential energy density $V(r_{bcp})$ at the bond critical point (3,-1). The relation between the hydrogen bond energy and potential energy density as [37]:

$$E_{HB} = V(r_{bcp})/2 \qquad (1)$$

In this equation the potential energy density is defined as:

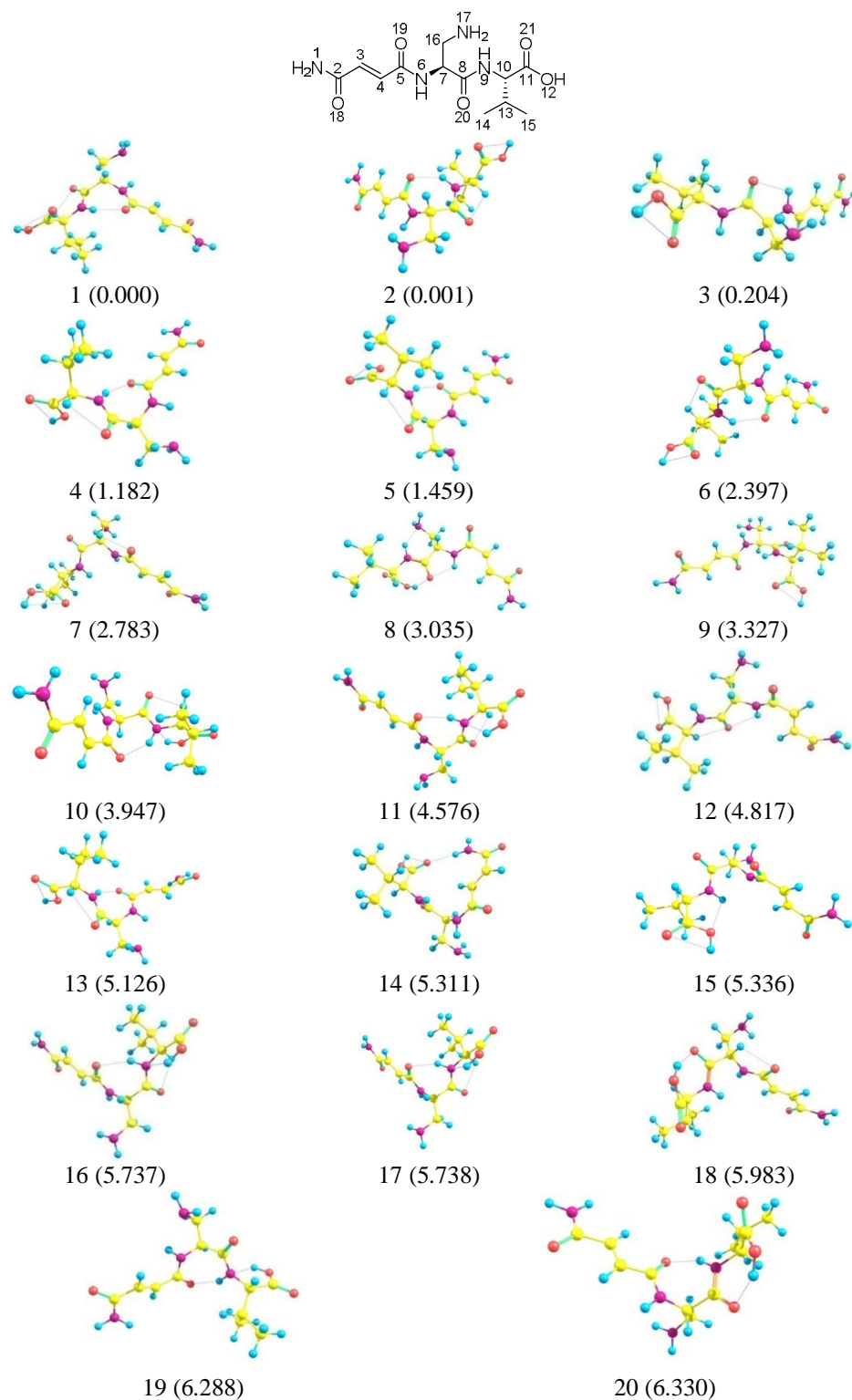$$V(\boldsymbol{r}_{cp}) = (h^2/4m)\nabla^2\rho(r_{cp}) - 2G(r_{cp}) \qquad (2)$$

In Eqs. (2) the $G(r)$ is Lagrangian kinetic energy density. The electron density is:

$$\rho(r) = \Sigma_i \, \eta_i \, |\varphi_i(r)|^2 = \Sigma_i \, \eta_i |\Sigma_i \, C_{l,i}\chi_i \, (r)|^2 \qquad (3)$$

where η_i is occupation number of orbital i, φ is orbital wavefunction, and χ is basis function. C is coefficient matrix, the element of the ith row jth column corresponds to the expansion coefficient of orbital j respect to basis function i. The gradient norm of electron density is defined as:

$$|\nabla\rho(r)| = [(\partial\rho(r)/\partial x)^2 + (\partial\rho(r)/\partial y)^2 + (\partial\rho(r)/\partial z)^2]^{1/2} \qquad (4)$$

1 (0.000)   2 (0.001)   3 (0.204)

4 (1.182)   5 (1.459)   6 (2.397)

7 (2.783)   8 (3.035)   9 (3.327)

10 (3.947)   11 (4.576)   12 (4.817)

13 (5.126)   14 (5.311)   15 (5.336)

16 (5.737)   17 (5.738)   18 (5.983)

19 (6.288)   20 (6.330)

Fig. 2. The most stable conformations and related energies. Energies are in kcal mol^{-1}, relative to the most stable conformation in the gas phase (structure 1). Yellow, blue, red, and purple coloured atoms are C, H, O and N, respectively.

The Laplacian of electron density is:

$$\nabla^2 \rho(r) = (\partial^2 \rho(r)/\partial x^2) + (\partial^2 \rho(r)/\partial y^2) + (\partial^2 \rho(r)/\partial z^2)$$

(5)

The positive and negative value of this function correspond to electron density which is depleted and locally concentrated, respectively.

The reduced density gradient (RDG) approach was used to study the non-covalent interaction [38]. The RDG can be used to study the weak interactions [39]. The RDG is defined as:

$$RDG(r) = [1 \div 2(3\pi^2)^{1/3}] \times [|\nabla \rho(r)| \div \rho(r)^{4/3}]$$

(6)

at which the $\rho(r)$ is as defined previously.

RESULTS AND DISCUSSIONS

The original structure of the dapdiamide D was created by Avogadro program and all of the chiral centers were checked to match with the original report. As mentioned in the computational method section, the Avogadro program was used to do conformational search. 83,365 structures were created by rotating the bonds to create different conformations. All of the structures were optimized with PM6 semi-empirical method. Eighty low-energy conformations were selected to be optimized by HF/6-311G(d) level of theory. Then, 40 of the structures were selected to be optimized using B3LYP/6-311+g(d,p) level of theory (The XYZ coordination of these optimized structures are available as supporting information). The frequency analysis was carried out to confirm the minimum character of the optimized structures (NIMG = 0). The above mentioned optimized structures were further analysed by MP2/6-311+g(d,p) level of theory to obtain single point energies. The selected twenty structures, with the lowest energy are presented in Fig. 2. The relative energies respect to the most stable conformation (structure 1) are presented in the parenthesis. Numbering method presented in Fig. 2 is used to present different data about the optimized structures.

To create hydrogen bond between a hydrogen atom and an acceptor atom such as O or N some criteria must be fitted. For example, the donor-hydrogen-acceptor angle must be greater than 110º and the distance between the mentioned atoms should be greater than the sum of their Van der Waals radii.

In most of the studied cases, an intramolecular hydrogen bonding between CO(5,19) and NH(9) is evident, leading to a boat-like seven-member ring. The distance between the oxygen of the carbonyl group and the hydrogen of the amide functional group in the mentioned ring is 2.0 Å (Table 1). The mentioned observation is presented in the structure 1 in Fig. 3a. Such behaviour is noticeable in the structures 2, 4-6, 10, 11, 13, 16, 17, 19 and 20.

In the structure 1, another five-member ring *via* the interaction between $NH_2(17)$ and NH(6) is noticeable (Fig. 3b). Such a ring is visible in the structures 2, 4-6, 10, 11, 13, 15 and 19, as well. The distance between $NH_2(17)$ and NH(6) is presented in Table 2. Comparison between Tables 1 and 2 makes us to conclude that the five-member rings in different structures are similar to each other.

As it was previously mentioned, in the structure 8, the seven-member ring is not visible. Further investigation of the structure 8 shows that another seven-member ring is recognizable (Fig. 3c).

The bond length for the CO functional groups is varying between 1.23, 1.22 and 2.24 Å for the structures 1, 3 and 8. The mentioned bond length in the structure 2 is 1.23 Å as well. The distance between $NH^{..}NH_2$ is 2.27, 2.25 and 2.26 Å for the structures 1, 2 and 10, respectively.

To further analyse the intramolecular interactions, natural bond orbital (NBO) studies were performed on the selected structures. Structures 1 and 8 are presented here as examples. In Fig. 4, interaction between LP(O31) with σ*(N13-H14) is presented. The other important intramolecular interaction is related to LP(N39) with σ*(N34-H35).

Selected intramolecular interactions in the structure 8 are studied using NBO point of view (Fig. 5). These interactions are related to LP(O33) with σ*(O28-H29), LP(O33) with σ*(N34-H35), and LP(N39) with σ*(N13-H14).

More analyses on the selected structures (1-10) were carried out using the Bader's atom in molecule (AIM) theory. In Fig. 6a, the critical points (3,-1) related to the

Table 1. Distance Between Oxygen of CO and Hydrogen of NH to Create a Boat-like Seven-member Ring
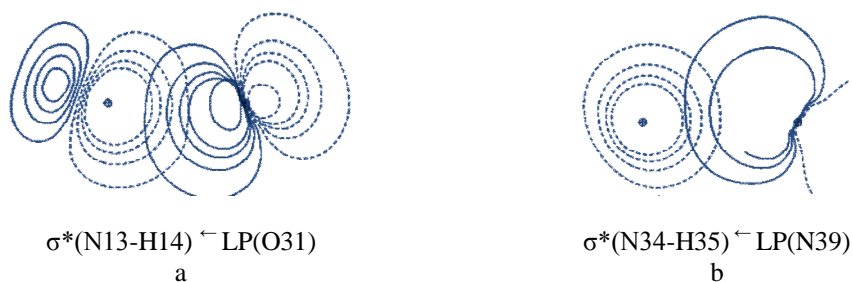
Entry	1	2	3	4	5	6	7	8	9	10	11
Structure no.	1	4	5	6	10	11	13	16	17	19	20
Distance (Å)	2.00	1.94	1.97	2.02	2.02	1.91	1.97	2.06	2.05	2.00	1.89

a   b   c
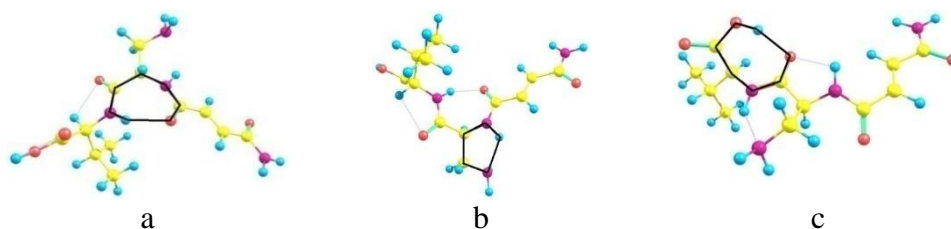
Fig. 3. Five- and seven-member rings.

Table 2. Distance Between Nitrogen of NH_2(17) and Hydrogen of NH(6) to Create a Five-member Ring

Structure no.	1	2	4	5	6	10	11	13	15	19
Distance (Å)	2.27	2.27	2.26	2.27	2.25	2.27	2.25	2.23	2.27	2.25

σ^*(N13-H14) $\leftarrow$ LP(O31) σ^*(N34-H35) $\leftarrow$ LP(N39)

a   b

Fig. 4. Interaction between a) LP(O31) with σ^*(N13-H14); b) LP(N39) with σ^*(N34-H35).

σ^*(O28-H29) $\leftarrow$ LP(O33)   LP(O33) $\rightarrow$ σ^*(N34-H35) σ^*(N13-H14) $\leftarrow$ LP(N39)

a   b   c
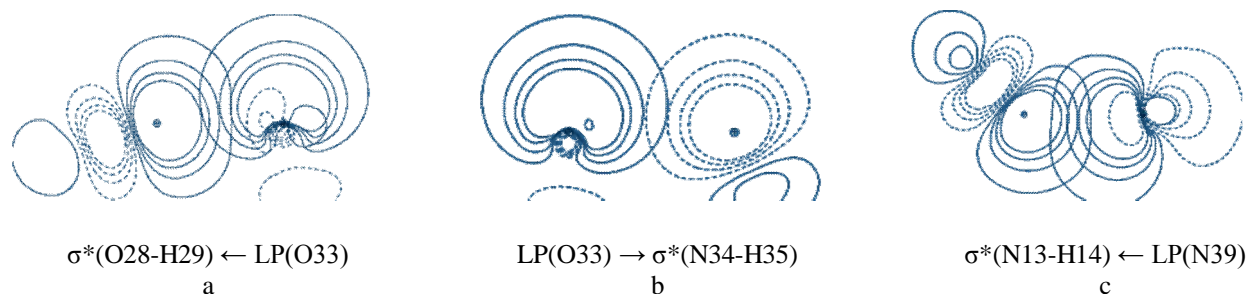
Fig. 5. Intramolecular interaction in the structure 8.

structure 1 are presented. Based on the AIM theory, (3,-1) critical point between each pair of nuclei is considered as "bond". From Fig. 6, it is obvious that, in addition to the regular bonds, other (3,-1) points are noticeable. Two of them are related to the NH and O/N atoms. These interactions, based on the electronegativity of the elements, can be considered as the hydrogen bonding. The other one is related to the interaction between CO and hydrogen of CH_3.

This interaction is not acceptable as a regular hydrogen bonding. To shed a light on this observation, further analysis was performed by considering the gradient-contour map with topology paths of electron density for the mentioned three interactions. Figure 6b shows the mentioned analysis for the CO···HN interaction. Clearly, a bonding between O and H is visible, as expected. Figure 6c reveals that the interaction between NH and NH_2 is not a
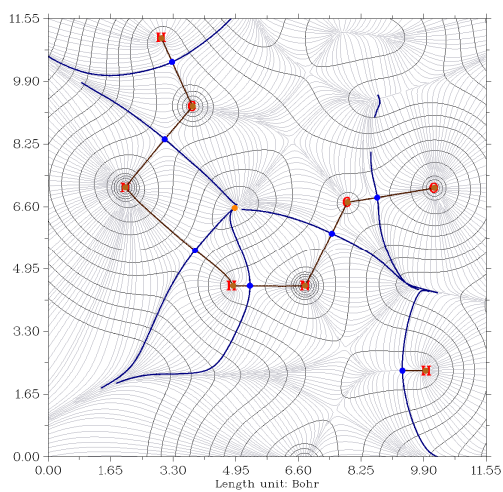

a

b
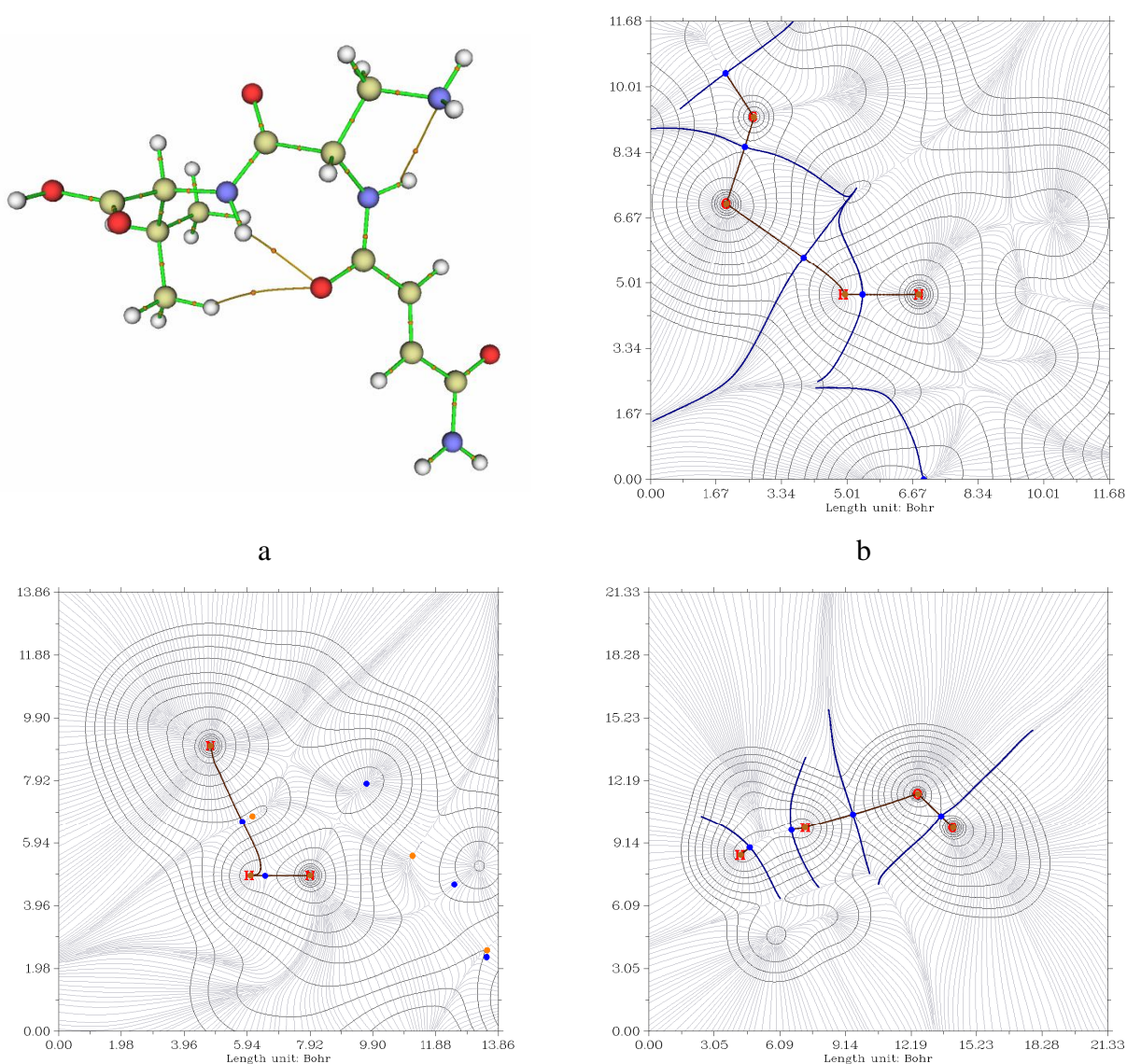
Fig. 6. (3,-1) points for the structure 1, based on the AIM theory. Brown, blue, and orange circles denote (3,-3), (3,-1), and (3,+1) critical points, respectively; bold dark-brown lines show the bond paths. The interbasin paths are presented by blue lines.
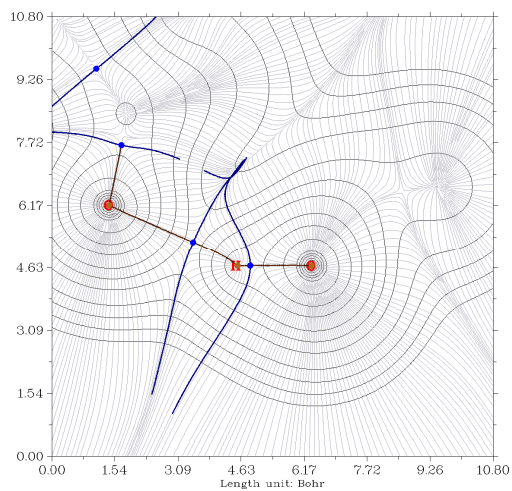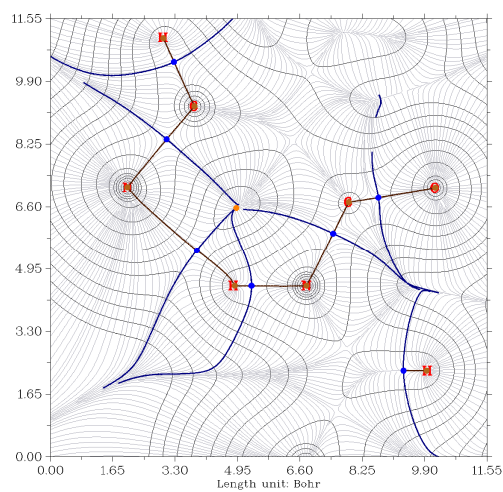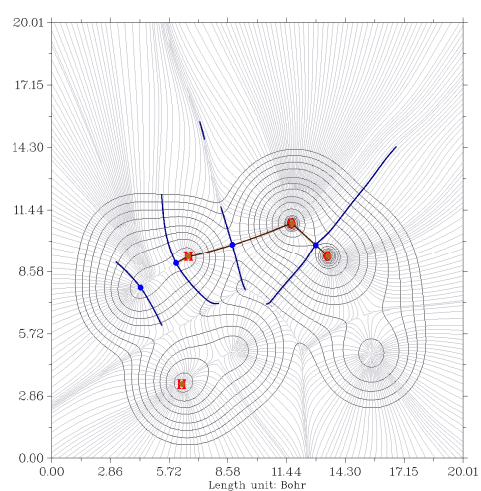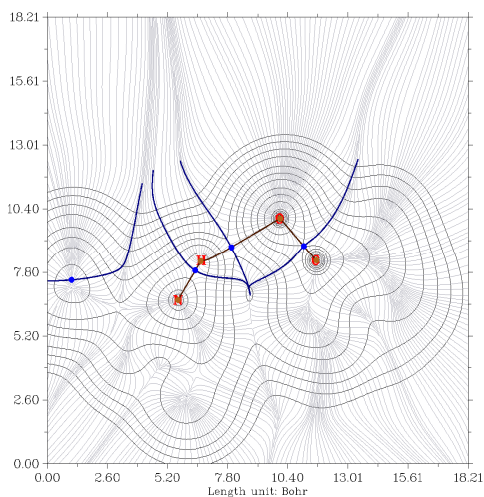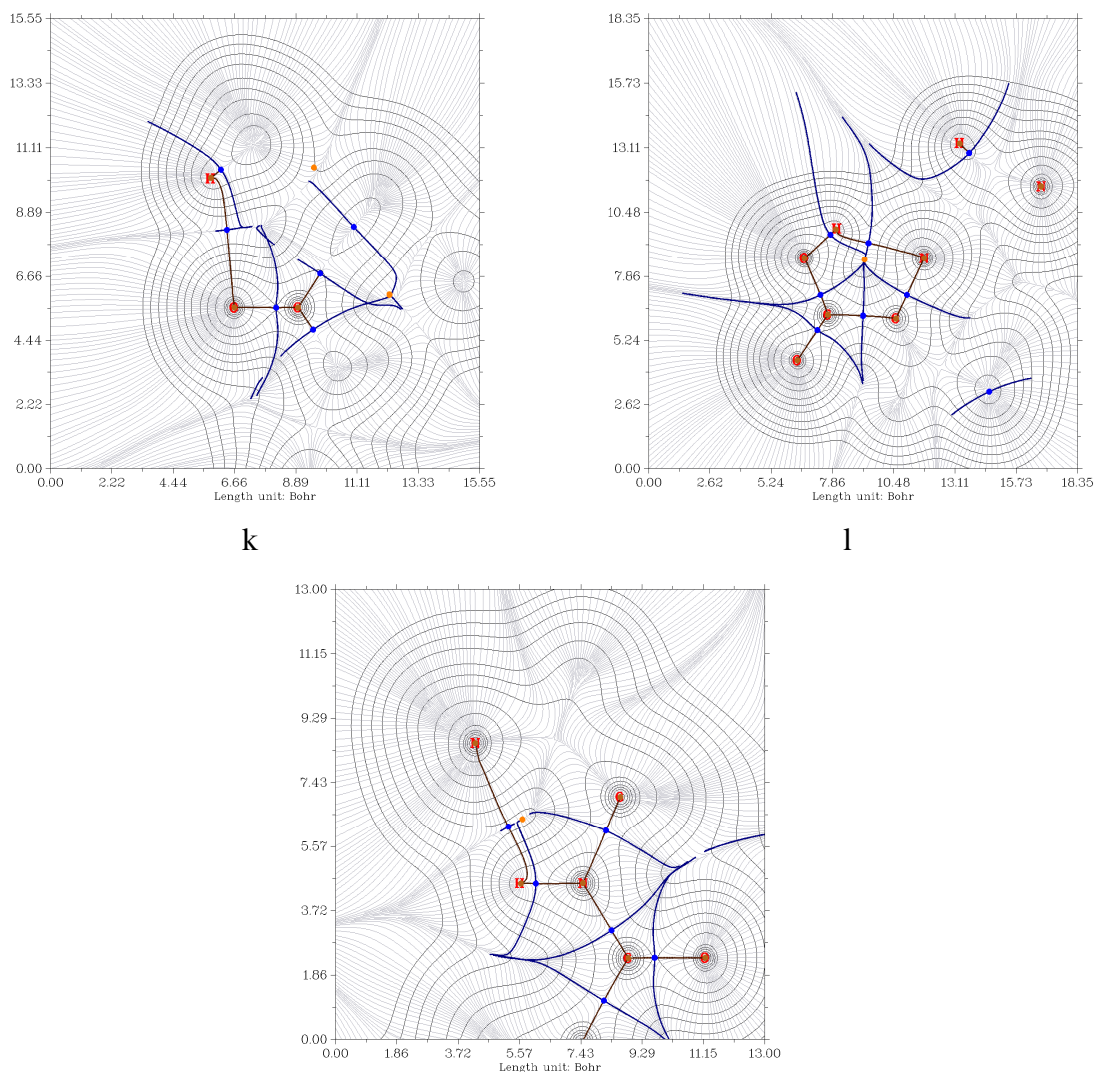
e
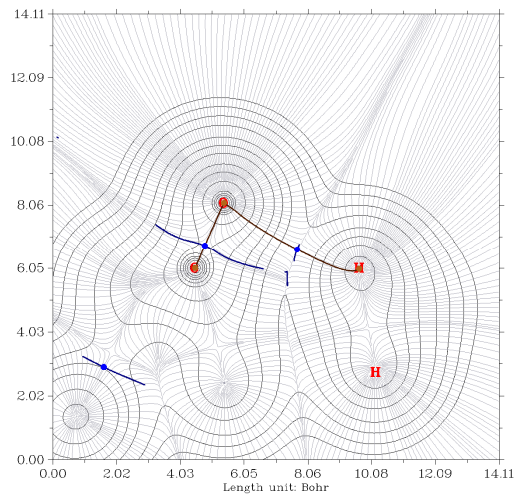
f


g

h

Fig. 6. Continued.

k

l

Fig. 6. Continued.

hydrogen bonding, although it was predicted in advance. No interbasin path is evident, however, Fig. 6d shows an interbasin path (blue line) between CO and H of the CH_3 group.

Considering the mentioned results, additional analysis is needed to conclude the identity of the observed interactions. Based on the Bader's QTAIM theory, an electron aggregation is noticeable in the (3,-1) critical point; it includes the chemical bond or atoms with attractive interactions. The (3,+1) type critical point indicates that the electron density is depleted at this point. This point displays the steric effect (non-bond overlap). The norm for

distinguishing (3,-1) and (3,+1) from each other is the second largest eigenvalue of Hessian matrix of electron density. If the mentioned value exceeds zero, the point is (3,+1); in the opposite situation, the point is (3,-1). In addition, there is positive correlation between the density of the electron and the strength of the weak interactions. Van der Waals interactions have very small electron density in the area of investigation, while in the strong steric interactions or hydrogen bonds, a relatively large amount of electron density is visible. Considering these two criteria simultaneously (sign of the second largest eigenvalue of Hessian matrix of electron density and electron density by
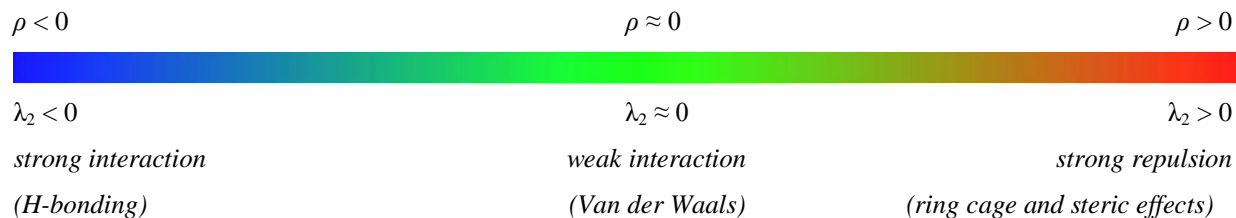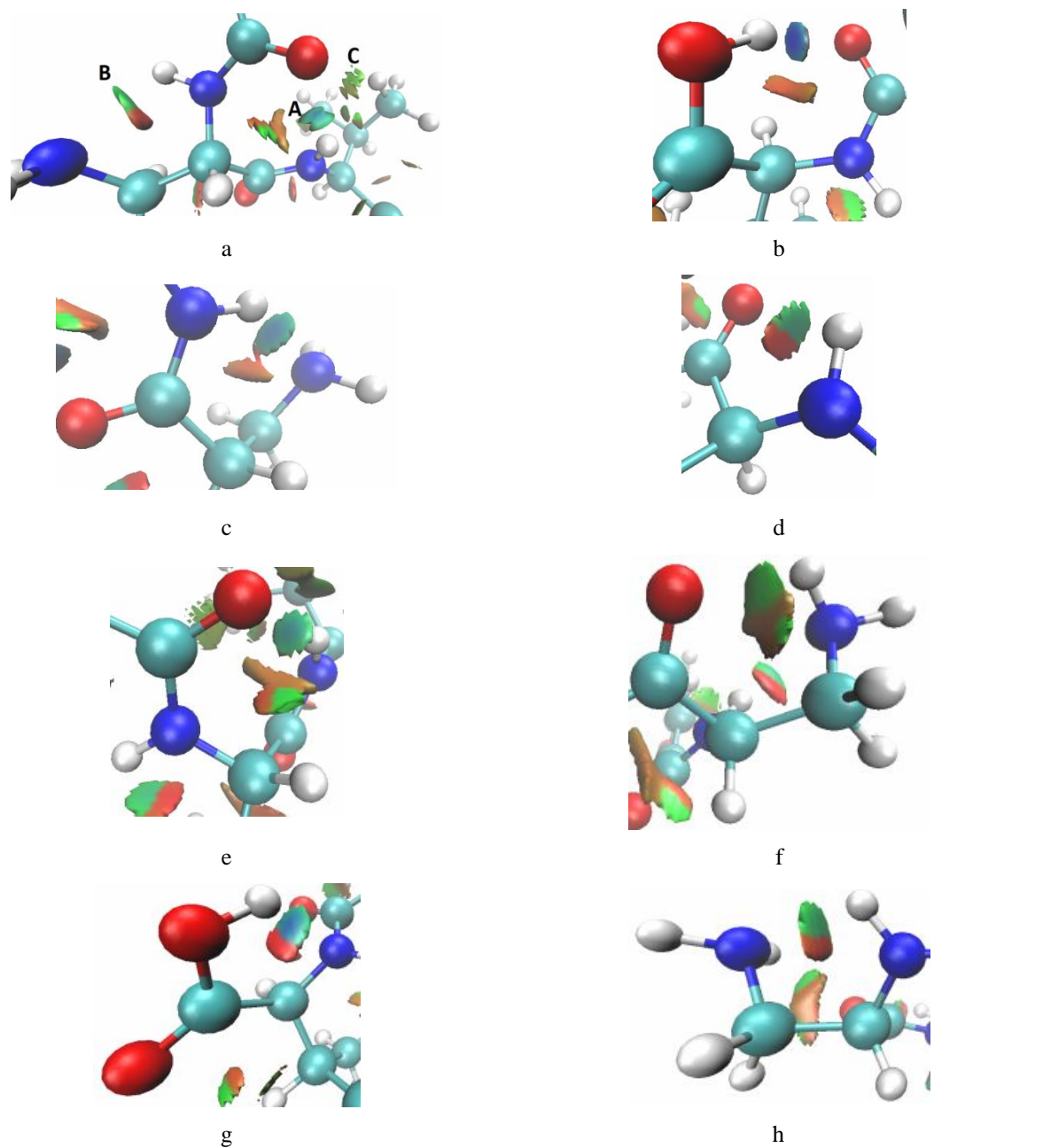
Fig. 7. The RDG isosurfaces related to the structure 1; Blue: Strong interaction such as hydrogen bonding; green: Van der Waals interactions; red: strong repulsion. [The mentioned colour definition is for the interactions; for atoms: deep blue: N; light blue: C; red: O; white: H].

its own) it is possible to analyse the interaction type. Therefore, the reduced density gradient (RDG) isosurfaces were subsequently used to investigate the previously mentioned interactions. In Fig. 7a, the RDG isosurfaces related to the intramolecular interactions in the structure 1 are presented. Three points are defined as A, B and C. In this graph, the region A, concerning to the interaction between CO and NH, is a hydrogen bonding and the regions B and C have Van der Waals nature.

Using the method suggested by Espinosa and co-workers, the energy of hydrogen bonds were calculated [35]. The mentioned method was used to calculate the hydrogen bonding energies for the selected structures. The energy of the hydrogen bonding related to CO and NH (seven-member ring) is -8.27 kcal mol^{-1}. The same method was used to calculate the energy of the NH$\cdots$NH$_2$ interaction (although it was regarded as Van der Waals interaction in the previous section). The calculated energy is -2.43 kcal; it is acceptable to consider this interaction as Van der Waals one.

The mentioned analyses were done for structures 2-10, as well. Results related to the bonds critical points for the structures 2-10 are presented in Fig. 8. The situation of the structure 2 is very similar to the structure 1 and the observed interactions are similar to the structure 1. The calculated energy for the hydrogen bonding between CO and NH is –5.42 kcal mol^{-1}, and for NH$\cdots$NH$_2$ is -2.43 kcal mol^{-1}. In the structure 4, the interactions are comparable with the structure 1, except the absence of interaction between CO and H of CH$_3$. The calculated energies based on the $V(r_{bcp})$ for the observed interactions are -6.28 and -4.10 kcal mol^{-1} for the CO$\cdots$NH and NH$\cdots$NH$_2$, respectively. The structure 5 is similar to the structure 4, and the structure 6 is comparable to the structure 2, again. The energies of the interaction in the structure 5 are -5.70 and -4.11 kcal mol^{-1}. The interaction energies for the structure 6 were calculated as -5.10 and -4.18 kcal mol^{-1}.

The structure 8 is completely different from the previous ones. In this structure, four interactions were predicted by the AIM analysis. The previously observed seven-member ring was missing and other kinds of interactions were introduced. NH$_2$ has contribution in a new interaction with NH group, next to the CO$_2$H functional group. The CO$_2$H has involvement in two interactions; one with CO and

another with CH$_3$. The mentioned CO group has another interaction with the NH group. Further studies of these interactions were carried out with considering the gradient-contour map with topology paths of electron densities. Figure 6e-h presents the interaction of OH of carboxylic acid with NH, CO of carboxylic acid with CH$_3$, NH with NH$_2$ and OH of carboxylic acid with CO, respectively. Clearly, the interaction between CO and CH$_3$ is not a hydrogen bonding, based on the interbasin paths. In other three interactions, the interbasin paths are noticeable. Extra examination of interactions was carried out by RDG isosurface analysis. The results are presented in Fig. 7b-d. From this figure, it is clear that the interactions presented as b and c are hydrogen bonding; while d is Van der Waals in nature. The energies related to these interactions were calculated as -8.93, -6.01 and -5.09 kcal mol^{-1} for the b, c and d, respectively.

In the structure 9 only one interaction between NH and N of amide functional group is visible. The interbasin analysis revealed that, this interaction is Van der Waals in nature. In the structure 10 five interactions based on the AIM analysis were clear. The gradient–contour maps with topology paths of electron densities for structure are shown in Fig. 6i-m. In this figure i-m refers to CO$\cdots$HNCO (amide), CO$\cdots$HCH$_2$ (methyl), CO$\cdots$HNH (amine), N$\cdots$HOCO (carboxylic acid), and NH$\cdots$NH$_2$, respectively. Considering the interbasins reveals that, except interaction j, in other interactions, hydrogen bonding is acceptable. To examine the nature of the interactions, the RDG isosurface study was carried out, as well. The results are presented in Fig. 7e-h.

In e and g the interactions are hydrogen bonding in nature. In f and h the interactions have Van der Waals identity. Considering these findings, the energies for the mentioned interactions (including the Van der Waals ones) are calculated to be -4.90, -2.48, -6.00 and -3.87 kcal mol^{-1}, correspondingly.

As mentioned previously, there is a correlation between the potential energy density $V(r)$ and the strength of the interactions. The quantities of $V(r)$ for top ten structures studied with AIM approach are presented in Table 3.

It can be seen that in the structure 1 the mentioned value has the highest amount for CO$\cdots$HN, while it is the least amount for CO$\cdots$H$_3$C. It was expected, because the
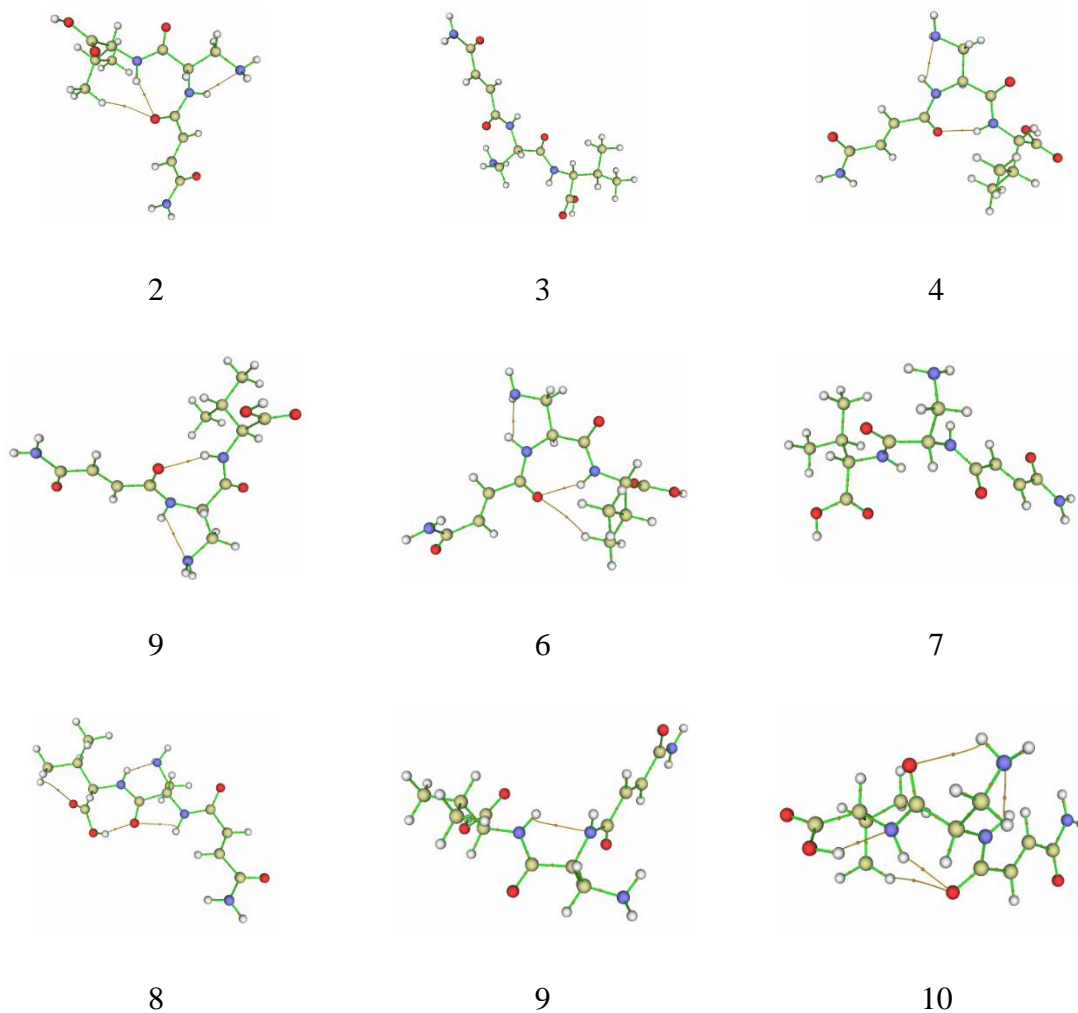
Fig. 8. (3,-1) points for the structures 2-10, based on the AIM theory.

interaction between CO⋯H₃C is Van der Waals in nature. The electron density in the critical point is obeying the same trend, as well. The Lagrangian kinetic energy $G(r)$ and Hamiltonian kinetic energy $K(r)$ are acting in similar manner and the highest amount is related to the CO⋯HN interaction. In the structure 2 exactly the same trend is visible. In the structure 3, only one critical point was calculated that concerns to CO⋯HN. The interaction between the mentioned atoms in this structure is weaker in comparison with the similar interactions in structures 1 and 2 based on the $V(r)$ criteria. The interaction between CO⋯HN in the structure 4 is stronger than other mentioned structures; while H₂N⋯HN in this structure is slightly weaker. Using the $G(r)$ and $K(r)$ as the determining criteria leads to the same results. In this structure, the electron density for CO⋯HN is higher than other two ones, in agreement with the strength predicted by $V(r)$. In the structure 5, between two critical points detected, CO⋯HN shows stronger interactions based on all of the mentioned criteria. Structure 6 is acting exactly similar to the structures 1, 2 and 4 and CO⋯HN is the strongest interaction. Structures 7 and 9 show similar behaviour and just one interaction is observable; H₂N⋯HN. Considering the mentioned norms, the strength of two interactions are

Table 3. Potential Energy Density V(r), Lagrangian Kinetic Energy G(r), Hamiltonian Kinetic Energy K(r), Density of Electrons, and Laplacian of Electron Density Calculated for the Selected Critical Points (Unit: a.u.)

Structure	Critical point: number and atoms	Density of electrons	Lagrangian kinetic energy G(r)	Hamiltonian kinetic energy K(r)	Potential energy density V(r)	Laplacian of electron density
	57 CO···H$_3$C	0.39×10^{-2}	0.29×10^{-2}	-0.83×10^{-3}	-0.21×10^{-2}	0.15×10^{-1}
1	69 CO···HN	0.25×10^{-1}	0.19×10^{-1}	0.74×10^{-3}	-0.19×10^{-1}	0.72×10^{-1}
	81 H$_2$N···HN	0.19×10^{-1}	0.16×10^{-1}	0.15×10^{-2}	-0.14×10^{-1}	0.70×10^{-1}
	57 CO···H$_3$C	0.40×10^{-2}	0.29×10^{-2}	-0.83×10^{-3}	-0.21×10^{-2}	0.15×10^{-1}
2	69 CO···HN	0.25×10^{-1}	0.19×10^{-1}	0.74×10^{-3}	-0.19×10^{-1}	0.72×10^{-1}
	81 H$_2$N···HN	0.19×10^{-1}	0.16×10^{-1}	-0.15×10^{-2}	-0.14×10^{-1}	0.70×10^{-1}
3	61 CO···HN	0.20×10^{-1}	0.18×10^{-1}	-0.21×10^{-2}	-0.16×10^{-1}	0.82×10^{-1}
	57 CO···H$_3$C	0.44×10^{-2}	0.33×10^{-2}	-0.88×10^{-3}	-0.24×10^{-2}	0.17×10^{-1}
4	65 CO···HN	0.28×10^{-1}	0.21×10^{-1}	0.88×10^{-3}	-0.22×10^{-1}	0.78×10^{-1}
	81 H$_2$N···HN	0.20×10^{-1}	0.16×10^{-1}	-0.14×10^{-2}	-0.15×10^{-1}	0.71×10^{-1}
5	76 CO···HN	0.26×10^{-1}	0.19×10^{-1}	0.87×10^{-3}	-0.20×10^{-1}	-0.74×10^{-1}
	66 H$_2$N···HN	0.19×10^{-1}	0.16×10^{-1}	-0.15×10^{-2}	-0.14×10^{-1}	0.70×10^{-1}
	57 CO···H$_3$C	0.43×10^{-2}	0.32×10^{-2}	-0.85×10^{-3}	-0.24×10^{-2}	0.16×10^{-1}
6	68 CO···HN	0.24×10^{-1}	0.18×10^{-1}	0.64×10^{-3}	-0.18×10^{-1}	0.69×10^{-1}
	81 H$_2$N···HN	0.20×10^{-1}	0.16×10^{-1}	-0.13×10^{-2}	-0.15×10^{-1}	0.70×10^{-1}
7	66 H$_2$N···HN	0.16×10^{-1}	0.14×10^{-1}	-0.25×10^{-2}	-0.12×10^{-1}	0.68×10^{-1}

Table 3. Continued

8	48 CO···H$_3$C	0.10×10^{-1}	0.84×10^{-2}	-0.14×10^{-2}	-0.70×10^{-2}	0.39×10^{-1}
	51 CO···HO	0.34×10^{-1}	0.25×10^{-1}	0.91×10^{-3}	-0.26×10^{-1}	0.98×10^{-1}
	66 CO···HN	0.21×10^{-1}	0.19×10^{-1}	-0.18×10^{-2}	-0.17×10^{-1}	0.84×10^{-1}
	82 H$_2$N···HN	0.29×10^{-1}	0.19×10^{-1}	0.16×10^{-2}	-0.21×10^{-1}	0.70×10^{-1}
9	66 HN···HN	0.17×10^{-1}	0.15×10^{-1}	-0.20×10^{-2}	-0.13×10^{-1}	0.66×10^{-1}
10	57 CO···H$_3$C	0.52×10^{-2}	0.38×10^{-2}	-0.88×10^{-3}	-0.29×10^{-2}	0.19×10^{-1}
	66 CO···HN	0.23×10^{-1}	0.17×10^{-1}	0.95×10^{-3}	-0.18×10^{-1}	0.65×10^{-1}
	80 CO···H$_2$N	0.19×10^{-2}	0.15×10^{-1}	-0.10×10^{-2}	-0.14×10^{-1}	0.65×10^{-1}
	83 H$_2$N···HN	0.12×10^{-1}	0.10×10^{-1}	-0.92×10^{-3}	-0.91×10^{-2}	0.44×10^{-1}

similar, although the structure 9 shows a slightly stronger interaction, which is evident from the higher amount of $V(r)$ and electron density. In the structures 8 and 10, four interactions are observable. In the structure 8, the CO···HO interaction is the strongest one from $V(r)$ point of view. In the structure 10, CO···HN plays the role of most important interaction.

CONCLUSIONS

In conclusion, a systematic theoretical study was carried out on the conformation space of the natural compound dapdiamide D. B3LYP/6-311+g(d,p) level of theory was used to optimize the structures. MP2/6-311+g(d,p) level of theory was used to calculate the single-point energies. The effects of the intramolecular interactions were studied. It was shown that five and/or seven-member rings are created *via* intramolecular hydrogen bonding or Van der Waals interactions. In most of the structures, an interaction between CO(5,19) and NH(9) is visible. This interaction creates a boat-like seven member ring. Another important intramolecular interaction is apparent from the interaction between NH2(17) and NH(6). This interaction forms a five-member ring. Based on the AIM studies, this interaction is Van der Waals in nature, although it was expected, derived from the electronegativity of the elements, to see a regular hydrogen bonding. In most of the structures, same pattern for the intramolecular interactions are noticeable.

ACKNOWLEDGMENTS

.

REFERENCES

[1]   Dawlaty, J.; Zhang, X.; Fischbach, M. A.; Clardy, J.

Dapdiamides, tripeptide antibiotics formed by unconventional amide ligases. *J. Nat. Prod.* **2010**, *73*, 441-446, DOI: 10.1021/np900685z.

[2] Brady, S. F.; Wright, S. A.; Lee, J. C.; Sutton, A. E.; Zumoff, C. H.; Wodzinski, R. S.; Beer, S. V.; Clardy, J. Pantocin B, an antibiotic from erwinia herbicola discovered by heterologous expression of cloned genes. *J. Am. Chem. Soc.* **1999**, *121*, 11912-11913, DOI: 10.1021/ja992790m.

[3] Jin, M.; Liu, L.; Wright, S. A. I.; Beer, S. V; Clardy, J. Structural and functional analysis of pantocin A: An antibiotic from pantoea agglomerans discovered by heterologous expression of cloned genes. *Angew. Chem. Int. Ed. Engl.* **2003**, *42*, 2898-2901, DOI: 10.1002/anie.200351053.

[4] Jin, M.; Fischbach, M. A.; Clardy, J. A biosynthetic gene cluster for the acetyl-CoA carboxylase inhibitor andrimid. *J. Am. Chem. Soc.* **2006**, *128*, 10660-10661, DOI: 10.1021/ja063194c.

[5] Hollenhorst, M. A.; Clardy, J.; Walsh, C. T. The ATP-dependent amide ligases DdaG and DdaF assemble the fumaramoyl-dipeptide scaffold of the dapdiamide antibiotics. *Biochemistry* **2009**, *48*, 10467-10472, DOI: 10.1021/bi9013165.

[6] Jin, M.; Wright, S. A. I.; Beer, S. V; Clardy, J. The biosynthetic gene cluster of pantocin a provides insights into biosynthesis and a tool for screening. *Angew. Chem. Int. Ed. Engl.* **2003**, *42*, 2902-2905, DOI: 10.1002/anie.200351054.

[7] Sutton, A. E.; Clardy, J. Synthesis and biological evaluation of analogues of the antibiotic pantocin B. *J. Am. Chem. Soc.* **2001**, *123*, 9935-9946, DOI: 10.1021/ja003770j.

[8] Kucharczyk, N.; Denisot, M. A.; Le Goffic, F.; Badet, B. Glucosamine-6-phosphate synthase from escherichia coli: Determination of the mechanism of inactivation by N3-fumaroyl-L-2,3-diaminopropionic derivatives. *Biochemistry* **1990**, *29*, 3668-3676, DOI: 10.1021/ bi00467a012.

[9] Milewski, S.; Andruszkiewicz, R.; Kasprzak, L.; Mazerski, J.; Mignini, F.; Borowski, E. Mechanism of action of anticandidal dipeptides containing inhibitors of glucosamine-6-phosphate synthase. *Antimicrob. Agents Chemother.* **1991**, *35*, 36-43, DOI: 10.1128/

AAC.35.1.36.

[10] Kalantari Fotooh, F.; Baharizadeh, M. Theoretical investigation of the effect of (8,0) single-walled Carbon nanotubes on acidity of aliphatic alcohols. *Phys. Chem. Res.* **2016**, *4*, 173-181.

[11] Razeghizadeh, A.; Rafee, V. Theoretical study of polyethylene crystallization using modified weighted density approximation (MWDA). *Phys. Chem. Res.* **2016**, *4*, 209-219.

[12] Shojaie, F. Theoretical studies of the vibrational spectra and molecular structures of dosulepin and doxepin. *Phys. Chem. Res.* **2016**, *4*, 245-270.

[13] Houshmand, F.; Jalili, S.; Schofield, J. Halogenated graphdiyne and graphyne single layers: A systematic study. *Phys. Chem. Res.* **2016**, *4*, 231-243.

[14] Yuguchi, Y.; Tran, V. T. T.; Bui, L. M.; Takebe, S.; Suzuki, S.; Nakajima, N.; Kitamura, S.; Thanh, T. T. T. Primary structure, conformation in aqueous solution, and intestinal immunomodulating activity of fucoidan from two brown seaweed species sargassum crassifolium and padina australis. *Carbohydr. Polym.* **2016**, *147*, 69-78, DOI: 10.1016/ j.carbpol.2016.03.101.

[15] Prashanth, J.; Reddy, B. V.; Rao, G. R. Investigation of torsional potentials, molecular structure, vibrational properties, molecular characteristics and NBO analysis of some bipyridines using experimental and theoretical tools. *J. Mol. Struct.* **2016**, *1117*, 79-104, DOI: 10.1016/j.molstruc.2016.03.062.

[16] Zhao, D.; Li, L.; He, D.; Zhou, J. Molecular dynamics simulations of conformation changes of HIV-1 regulatory protein on graphene. *Appl. Surf. Sci.* **2016**, *377*, 324-334, DOI: 10.1016/j.apsusc.2016.03.177.

[17] Rode, J. E.; Narbutt, J.; Dudek, M. K.; Kaźmierski, S.; Dobrowolski, J. C. On the conformation of the actinide-selective hydrophilic SO_3-Ph-BTP ligand in aqueous solution. A computational study. *J. Mol. Liq.* **2016**, *219*, 224-231, DOI: 10.1016/ j.molliq.2016.02.085.

[18] Arabieh, M.; Karimi-Jafari, M. H.; Ghannadi-Maragheh, M. Low-energy conformers of pamidronate and their intramolecular hydrogen bonds: A DFT and QTAIM study. *J. Mol. Model.* **2013**, *19*, 427-438, DOI: 10.1007/s00894-012-1564-3.

[19] Reva, I. .; Stepanian, S. .; Adamowicz, L.; Fausto, R. Missing conformers. Comparative study of conformational cooling in cyanoacetic acid and methyl cyanoacetate isolated in low temperature inert gas matrixes. *Chem. Phys. Lett.* **2003**, *374*, 631-638, DOI: 10.1016/S0009-2614(03)00782-6.

[20] Dowd, M. K.; Kiely, D. E.; Zhang, J. Monte carlo-based searching as a tool to study carbohydrate structure. *Carbohydr. Res.* **2011**, *346*, 1140-1148, DOI: 10.1016/j.carres.2011.04.013.

[21] Lee, J.; Scheraga, H. A.; Rackovsky, S. New optimization method for conformational energy calculations on polypeptides: Conformational space annealing. *J. Comput. Chem.* **1997**, *18*, 1222-1232, DOI: 10.1002/(SICI)1096-987X(19970715)18:9< 1222::AID-JCC10>3.0.CO;2-7.

[22] De Pol, S.; Zorn, C.; Klein, C. D.; Zerbe, O.; Reiser, O. Surprisingly stable helical conformations in alpha/beta-peptides by incorporation of cis-beta-aminocyclopropane carboxylic acids. *Angew. Chem. Int. Ed. Engl.* **2004**, *43*, 511-514, DOI: 10.1002/ anie.200352267.

[23] Hill, D. J.; Mio, M. J.; Prince, R. B.; Hughes, T. S.; Moore, J. S. A field guide to foldamers. *Chem. Rev.* **2001**, *101*, 3893-4012, DOI: 10.1021/cr990120t.

[24] Gellman, S. H. Foldamers: A manifesto. *Acc. Chem. Res.* **1998**, *31*, 173-180, DOI: 10.1021/ar960298r.

[25] Seebach, D.; Matthews, J. L. β-Peptides: A surprise at every turn. *Chem. Commun.* **1997**, No. 21, 2015-2022, DOI: 10.1039/a704933a.

[26] Pang, R.; Guo, M.; Ling, S.; Lin, Z. Thorough theoretical search of conformations of neutral, protonated and Deprotonated glutamine in gas phase. *Comput. Theor. Chem.* **2013**, *1020*, 14-21, DOI: 10.1016/j.comptc.2013.07.016.

[27] Ramaniah, L. M.; Kamal, C.; Kshirsagar, R. J.; Chakrabarti, A.; Banerjee, A. How universal are hydrogen bond correlations? A density functional study of intramolecular hydrogen bonding in low-energy conformers of α-amino acids. *Mol. Phys.* **2013**, *111*, 3067-3076, DOI: 10.1016/j.comptc.2013.07.016.

[28] Kuhn, B.; Mohr, P.; Stahl, M. Intramolecular hydrogen bonding in medicinal chemistry. *J. Med.* *Chem.* **2010**, *53*, 2601-2611, DOI: 10.1021/jm100087s.

[29] Hanwell, M. D.; Curtis, D. E.; Lonie, D. C.; Vandermeersch, T.; Zurek, E.; Hutchison, G. R. Avogadro: An advanced semantic chemical editor, visualization, and analysis platform. *J. Cheminform.* **2012**, *4*, 1-17, DOI: 10.1186/1758-2946-4-17.

[30] Frisch, M. J.; Trucks, G. W.; Schlegel, H. B.; Scuseria, G. E.; Robb, M. A.; Cheeseman, J. R.; Scalmani, G.; Barone, V.; Mennucci, B.; Petersson, G. A.; et al. Wallingford, CT, USA 2009, Gaussian 09 (Rev. A01), Gaussian, Inc., Wallingfor.

[31] Korth, H. -G.; de Heer, M. I.; Mulder, P. A DFT study on intramolecular hydrogen bonding in 2-substituted phenols: Conformations, enthalpies, and correlation with solute parameters. *J. Phys. Chem. A* **2002**, *106*, 8779-8789, DOI: 10.1021/jp025713d.

[32] Legault, C. CYLview. 2009, p www.cylview.org.

[33] Lu, T.; Chen, F. Multiwfn: A multifunctional wavefunction analyzer. *J. Comput. Chem.* **2012**, *33*, 580-592, DOI: 10.1002/jcc.22885.

[34] Lu, T.; Chen, F. Quantitative analysis of molecular surface based on improved marching tetrahedra algorithm. *J. Mol. Graph. Model.* **2012**, *38*, 314-323, DOI: 10.1016/j.jmgm.2012.07.004.

[35] Bader, R. F. W. *Atoms in Molecules: A Quantum Theory*; Clarendon Press, 1994.

[36] Bader, R. F. W. Atoms in molecules. *Acc. Chem. Res.* **1985**, *18*, 9-15, DOI: 10.1021/ar00109a003.

[37] Espinosa, E.; Molins, E.; Lecomte, C. Hydrogen bond strengths revealed by topological analyses of experimentally observed electron densities. *Chem. Phys. Lett.* **1998**, *285*, 170-173, DOI: 10.1016/S0009-2614(98)00036-0.

[38] Saleh, G.; Gatti, C.; Lo Presti, L. Non-covalent interaction via the reduced density gradient: independent atom model vs. experimental multipolar electron densities. *Comput. Theor. Chem.* **2012**, *998*, 148-163, DOI: 10.1016/j.comptc.2012.07.014.

[39] Johnson, E. R.; Keinan, S.; Mori-Sánchez, P.; Contreras-García, J.; Cohen, A. J.; Yang, W. Revealing noncovalent interactions. *J. Am. Chem. Soc.* **2010**, *132*, 6498-6506, DOI: 10.1021/ja100936w.